Acousto-optic multifrequency modulators: reduction of the phase-grating intermodulation products

M. G. Gazalet, J. C. Kastelik, C. Bruneel, O. Bazzi, and E. Bridoux

The multifrequency acousto-optic modulator efficiency is limited mainly by the two-tone, third-order intermodulation products. We show here that a suitable anisotropic interaction can greatly reduce this undesirable effect. Numerical computations have been drawn for a paratellurite acousto-optic cell, and it is shown that a reduction of ~ 16 dB can be reached, limited by the acoustic nonlinearity intermodulation products. A specific method for experimental validation, based on optical heterodyning on a photodetector, is presented. The experimental results agree well with the theoretical ones.

Key words: Acousto-optics, intermodulations.

Introduction

It is well known that two main effects contribute to the limitations in multifrequency acousto-optic diffraction: the acousto-optic rediffraction phenomenon described by the phase-grating theory[1] and the acoustic nonlinearities in the propagation medium.[2] Both effects have been studied extensively[3–5] and lead to cross talk and intermodulation. Among all the intermodulation products the two-tone third orders appear as the more constraining ones, since their frequency spectra lie in the useful bandwidth of the acousto-optic cell.

When the acousto-optic device is used to split a coherent light beam angularly into N regularly spaced, independently modulated fractions, the acoustic wave consists of N harmonic carriers lying in the acousto-optic frequency bandwidth with a proper amplitude modulation. In such a situation, when N is not large (typically 2–8), we show that the phase-grating intermodulation products can be greatly reduced in anisotropic interaction compared with the isotropic case, allowing much higher interaction efficiencies, limited only by the acoustic nonlinearities.

In this paper, after a brief description of the two classical sources of intermodulation products, we present in some detail the basic principle of the reduction of phase-grating intermodulation products. A numerical study has been carried out on a paratellurite acousto-optic cell. For experimental verification purposes a practical device has been realized. An original heterodyne method has been developed and is used to measure the magnitude of intermodulation products.

The authors are with Institut d'Électronique et de Microélectronique du Nord, Départment Opto-Acousto-Électronique, Université de Valenciennes, B. P. 311, 59304 Valenciennes Cedex, France.

Received 31 December 1991.
0003-6935/93/132455-06$05.00/0.

Phase-Grating Intermodulation Products Versus Acoustic Nonlinearity Effects

Multiple Rediffractions

This phenomenon has been described by Hecht.[1] The analytical results have been studied in two limiting cases: the Raman–Nath regime and the Bragg regime.[6]

In the particular case of the Bragg regime the light intensity is diffracted in only one direction by a monochromatic acoustic wave. It is then preferred since the acousto-optic efficiency η may reach large values. Only this Bragg interaction is considered in this paper. In this situation the phase-grating intermodulation products caused by multiple rediffractions are illustrated in Fig. 1, where for simplicity only two acoustic frequencies, f_1 and f_2, have been considered. The different orders involved in the interaction are identified by their optical frequencies. The incident light beam (frequency ν_0) is diffracted by the two acoustic waves with deflection angles proportional to the acoustic frequencies (f_1 and f_2). They may be rediffracted in the reverse direction, leading to the two second intermodulation orders with a corresponding reduction in the intensity of the two princi-

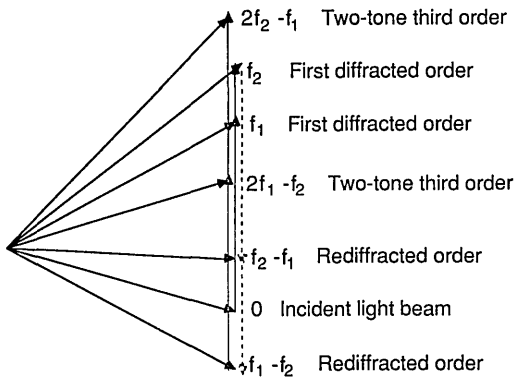

Fig. 1. Acousto-optic intermodulation modes pattern.

pal diffracted orders. A third-order rediffraction may then occur and is denoted as a two-tone third intermodulation order.

When the acoustic wave consists of N carriers, regularly frequency spaced by δf, the two-tone, third-order diffraction caused by f_1 and $f_1 + \delta f$ lies in the same directions as the useful first-order direction caused by other carriers at frequencies $f_1 - \delta f$ and $f_1 + 2\delta f$. The two-tone third orders are often considered more troublesome than the second orders, since they may not be spatially filtered.

The main result derived by Hecht[1] is that the intensities of the acousto-optic rediffraction intermodulation products depend only on the first-order efficiencies. In the particular case of synchronous phase matching[7] for all interactions (including second- and third-order rediffractions), Hecht has shown that in the small-signal approximation the two-tone, third-order efficiency η' is given by

$$\eta' = \eta^3/36, \tag{1}$$

where η is the first-order undepleted efficiency for each of the two first orders.

Acoustic Nonlinear Effects

It is well known that the nonlinearity of the medium leads to the generation of harmonics when a monochromatic acoustic wave propagates inside the material.[8] If the acoustic wave consists, as described above, of the sum of monochromatic carriers, in addition to these harmonics, acoustic intermodulation products are generated with a linear combination of the emitted fundamental frequencies.

It may be shown[2] that, in the small-signal approximation, the acousto-optic efficiency η'' for a nonlinearly generated two-tone, third-order acoustic wave is given by

$$\eta'' = C\eta^3, \tag{2}$$

where η is, as in Eq. (1), the first-order undepleted efficiency for each of the two first orders and C is a constant depending on the following:

(1) The propagation medium (nonlinear acoustic coefficients, acousto-optic figure of merit, etc.).

(2) Fundamental frequencies.

(3) The optical wavelength λ.

(4) The acoustical power density, which for fixed η depends on the transducer width W parallel to the propagation direction, i.e., the constant C will depend on the acousto-optic frequency bandwidth Δf of the Bragg cell.

(5) Since the acoustic intermodulation products grow along the propagation direction, C will also depend on the propagation time τ between the emitting acousto-electric transducer and the acousto-optic interaction region.

Practical Bragg Cell

In practice both spurious effects are present. A comparison of their relative importance is described better by the dynamic range α, defined as

$$\alpha = 10 \log(\eta/\eta_s)\text{dB}, \tag{3}$$

where η_s is the spurious efficiency, which may be assumed to be nearly equal to the higher value of η' and η''. The general behavior of the dynamic range versus propagation time at constant efficiency is shown in Fig. 2. The hatched region corresponds to a forbidden zone that cannot be reached by the incident light wave caused by the angular tilt of the Bragg cell. Near the transducer the nonlinear acoustic effects are negligible, and the dynamic range is mainly limited by acousto-optic phase-grating-theory intermodulation products, and the opposite situation occurs far from it. For high efficiencies the spurious orders can no longer be derived from Eq. (1), and their magnitudes are derived from the numerical solution of the usual coupled-wave equations describing the multifrequency acousto-optic interaction.

Reduction of the Phase-Grating Intermodulation Products in Anisotropic Interaction

The isotropic Bragg interaction is a symmetrical one, i.e., the acousto-optic frequency bandwidth remains unchanged if the incident and diffracted rays are swapped. This is due to the symmetrical form of the wave-vector diagram [Fig. 3(a)] and is not the case in anisotropic interaction [Fig. 3(b)]. The behavior of the acousto-optic efficiency versus frequency is directly related to the wave-vector mismatch Δk or

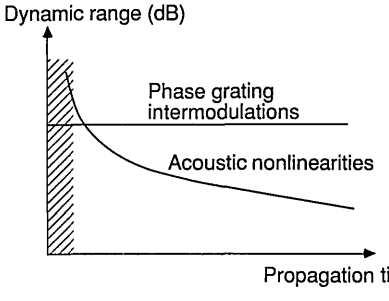

Fig. 2. General behavior of the dynamic range versus the propagation time at constant efficiency.

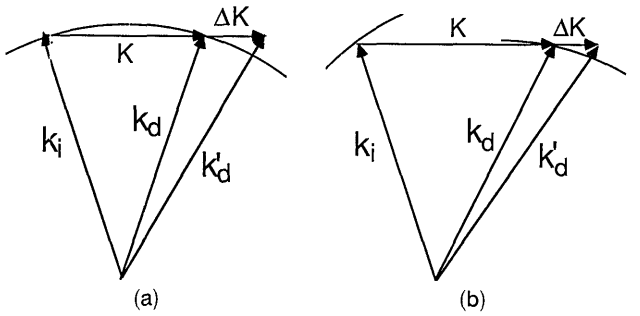

Fig. 3. (a) Isotropic Bragg symmetrical interaction wave-vector diagram. (b) Anisotropic interaction wave-vector diagram.

more exactly to the phase mismatch $\Delta\phi$ (Ref. 7):

$$\Delta\phi = \Delta k W, \tag{4}$$

the efficiency η being a decreasing function in $\Delta\phi$.

The two-tone, third-order efficiency η' [Eq. (1)] has been derived by Hecht under the assumption that the $\Delta\phi$ values were negligible for all the considered useful or spurious orders, whether they lie in the direct bandwidth (direct phase mismatch $\Delta\phi_d$) or in the vicinity of the incident light wave (inverse phase mismatch $\Delta\phi_i$). In what follows we consider an anisotropic interaction; the direct bandwidth is denoted Δf and the frequency separation δf between the N acoustic carriers is given by

$$\delta f = \Delta f / N. \tag{5}$$

We shall assume as usual that $\Delta\phi_d = 0$, but the assumption $\Delta\phi_i = 0$ will not be retained since the inverse wave-vector mismatch may reach large values for the considered anisotropic interaction.

Figure 4 shows the wave-vector diagram corresponding to the above approximation in the simplest case $N = 2$. Seven light orders have been considered in this two-tone, third-order evaluation. An indexed notation is adopted here according to the following scheme:

(1) Incident and first diffracted orders will support only one suffix, 0 for the incident undiffracted ray, 1 or 2 according to the wave vector $\mathbf{K}_1$ and $\mathbf{K}_2$ involved in the considered diffraction.

(2) Rediffracted orders are denoted by two suffixes in parentheses; order (1, 2) is the rediffraction from order 1 by the acoustic wave vector $\mathbf{K}_2$, and order (2, 1) is the rediffraction from order 2 by the acoustic wave vector K_1.

(3) Similarly the two-tone third orders are denoted by three indices in parentheses (1, 2, 1) and (2, 1, 2).

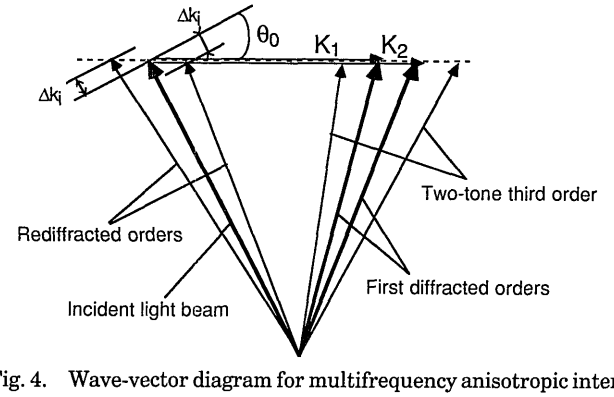

Fig. 4. Wave-vector diagram for multifrequency anisotropic interaction assuming direct phase mismatch $\Delta\phi_d = 0$.

The wave-vector mismatches for all direct diffractions are assumed to be perfectly negligible, while the rediffraction wave surface is approximated by its linear tangent, leading to inverse wave-vector mismatches Δk_i proportional to the angles between the considered rediffracted order and the zeroth incident one. That is, the inverse phase mismatch $\Delta\phi_i$ is

$$\Delta\phi_i = 2\pi\delta f W\theta_0 / v, \tag{6}$$

where v is the acoustic velocity and θ_0 is the angle between the acoustic wave vector and the tangent to the optical surface.

The rediffractions may be considerably reduced by the nonzero phase mismatches, and consequently the phase-grating dynamic range will be proportionally raised. Our aim is to evaluate the needed value of $\Delta\phi_i$ to reduce sufficiently the phase-grating intermodulation products and to reach the dynamic range caused by the acoustical nonlinear effects. This may be represented graphically (see Fig. 2): For the minimal realizable value τ_{min} from practical considerations, the dynamic range of the phase-grating intermodulation products should be raised by the proposed method up to at least the acoustic nonlinearity dynamic range at the same τ_{min}. This limiting case will be reached for a threshold value $\Delta\phi_t$ of the inverse phase mismatch. The required values for $\Delta\phi_i$ being large, this justifies neglecting the higher-order rediffractions.

Numerical Computation for a Paratellurite Shear-Wave Acousto-Optic Modulator

The paratellurite (TeO_2) crystal is often used for acousto-optic purposes. This is due mainly to the existence of a particularly slow shear wave [$\sim$650 m/s (Ref. 9)], propagating along the [110] crystal axis, leading to a very high figure of merit ($M_2 = 1, 2 \times 10^{-12}$ s^3/kg). Moreover the acoustic nonlinearity effects are considerably lowered, since they are due only to fourth-order elastic constants, the third-order constants being identically zero because of symmetry considerations.

A numerical computation has been drawn with the formalism of the coupled-wave equations.[10] For the clearest comparison with previously reported results[1,2] we assumed two acoustic carriers with exact phase-matching direct interaction ($\Delta\phi_d = 0$). The basic equation for this particular interaction condition is given in Appendix A. Seven light orders have been considered as described in Fig. 4. The dynamic

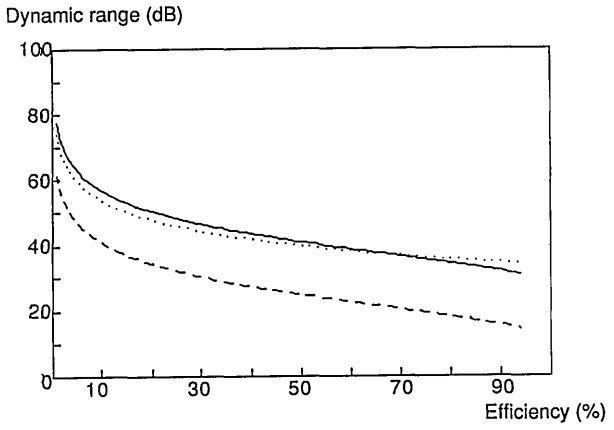

Fig. 5. Dynamic range versus acousto-opotic efficiency. Effect of the inverse basic phase mismatch. Comparison with the acoustic nonlinearities: ——, phase-grating intermodulation with $\Delta\phi_i = 6\pi$; – – –, phase-grating intermodulation with $\Delta\phi_i = 0$; ....., acoustic nonlinearities.

range is calculated from Eq. (3) with

$$\frac{\eta}{\eta_S} = \left|\frac{g_1}{g_{(1,2,1)}}\right|^2 = \left|\frac{g_2}{g_{(2,1,2)}}\right|^2. \tag{7}$$

The acousto-optic phase-grating dynamic range has been evaluated as a function of the total acousto-optic efficiency for different fixed values of the inverse basic phase mismatch $\Delta\phi_i$. Figure 5 represents the results for the particular value $\Delta\phi_i = 0$, corresponding to the Hecht limiting case and a large value $\Delta\phi_i = 6\pi$. For comparison the acoustic nonlinear dynamic range as evaluated by Elston is also reported (assuming a minimal value $\tau_{min} = 0.5$ μs). The phase-grating dynamic range is shown to be enhanced by ~16 dB because of the reduction of the inverse bandwidth associated with the increase of $\Delta\phi_i$ and is now near the acoustic nonlinearity limiting value.

The threshold value $\Delta\phi_t$ of the $\Delta\phi_i$ parameter, defined so that the two dynamic range limitations become equal, is then evaluated. Figure 6 represents the $\Delta\phi_t$ parameter as a function of the total acousto-optic efficiency.

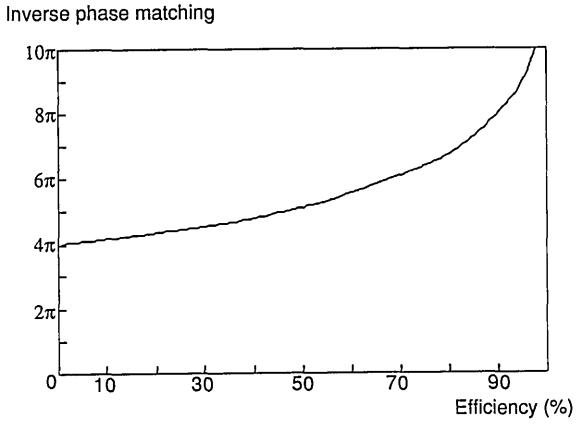

Fig. 6. Threshold value for the inverse phase mismatch versus acousto-optic efficiency.

Experimental Validation

For an accurate measurement of the two-tone-order light intensity, the effect of spurious light components diffused in the same direction must be eliminated. Since these two light frequencies are different, they may be distinguished in the heterodyne configuration shown in Fig. 7. The He–Ne laser is focused by lens L1 into the multiple-frequency paratellurite acousto-optic modulator (MFAOM) under test. The waist of the Gaussian beam is nearly 150 μm in the interaction region. The spatial filter S selects either the (1, 2, 1) or (2, 1, 2) intermodulation order together with some diffused light. A small fraction of the laser beam is separated by the beam splitter BS1 and focused by the same lens L1 into the additional paratellurite acousto-optic modulator (AOM). The spatial filter S′ isolates the diffracted order. Lenses L2 and L′2 image the interaction regions of MFAOM and AOM, respectively, on the beam splitter BS2 used for recombination. The two light components are then focused on the photodetector PD by lens L3; a beat electric signal results from the heterodyne effect.

The associated electronic system consists of three phase locked loops, an adder and two amplifiers. The two main carriers with adjustable frequencies f_1 and f_2 are generated by the two phase locked-loop oscillators, PLL1 and PLL2, respectively. The $\Delta\phi_i$ value is proportional to the difference between the two frequencies, $\delta f = f_2 - f_1$, according to Eq. (6). These two frequencies are chosen to be symmetrical about the central frequency f_0 of the MFAOM. This is summarized as follows:

$$f_1 = f_0 - \delta f/2, \tag{8a}$$

$$f_2 = f_0 + \delta f/2. \tag{8b}$$

The two carriers are then amplified, added, and applied to the electromechanical transducer in the MFAOM. The electronically generated intermodulation products have been measured and shown to be at

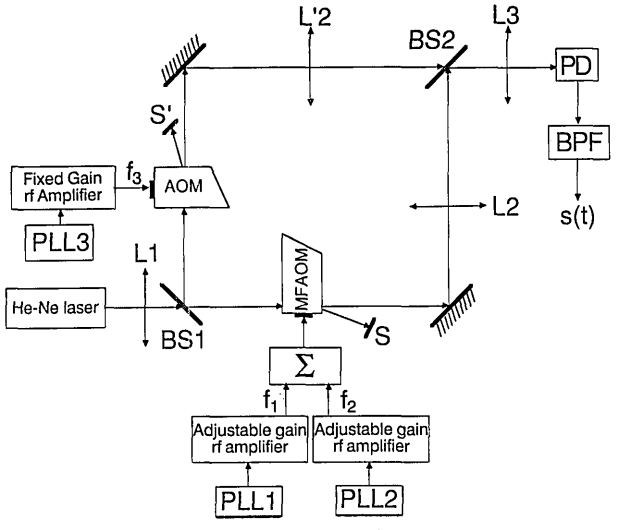

Fig. 7. Experimental setup.

least 10 dB beyond the theoretical prediction for the acousto-optic two-tone, third-order dynamic range. The intensity of the acousto-optic, two-tone, third-order diffracted beam is low and may be of the same order of magnitude as the spurious diffused light. For a precise measurement of the intermodulation products, a third carrier with frequency f_3 is applied to the additional AOM. The frequency f_3 is chosen to be close to either $2f_2 - f_1$ or $2f_1 - f_2$ frequencies:

$$f_3 = 2f_1 - f_2 \pm f_b, \tag{9a}$$

$$f_3 = 2f_2 - f_1 \pm f_b. \tag{9b}$$

Equations (9a) and (9b) hold for, respectively, (1, 2, 1) and (2, 1, 2) two-tone, third-order measurements, and f_b is a fixed frequency shift. This results in a beat at this same frequency f_b on the photodetector and is used to differentiate statically diffused light from the two-tone third order. The useful signal $s(t)$ can be extracted by proper bandpass filtering (BPF) with central frequency f_b. The amplitude s_{max} of the sinusoidal beat signal $s(t)$ is proportional to $(\eta_3\eta_S)^{1/2}$, where η_3 is f_3 depending on the acousto-optic efficiency of the AOM and η_S is the spurious efficiency to be measured. A calibration step with a known single diffracted intensity from the MFAOM is then necessary to establish the correspondence between s_{max}, f_3, and η_s.

This experimental setup has been realized with a beat frequency f_b of 1 MHz. The quartz BPF has the same center frequency of 1 MHZ, and a ±1-kHz shift about this frequency corresponds to more than 30-dB attenuation. The TeO_2 tangential phase-matching MFAOM has been realized with a crystal cut θ_a (as defined by Yano *et al.*[11]). According to the incidence direction, there are two possible wave-vector configurations leading to identical acousto-optic frequency bandwidths with different central frequencies f_+ anf f_- (Ref. 12) for the same value of θ_a. A central frequency f_+ of 75 MHz, equal to that used by Elston,[2] is reached with a crystal cut $\theta_a = 3.6°$. This corresponds to $v = 625$ m/s and $\theta_0 = 1.26°$. The transducer length W is 4 mm, corresponding to an acousto-optic 3-dB frequency bandwidth Δf of 50 MHz. The inverse phase mismatch $\Delta\phi_i$ has been varied from π to 8π. The lower bound is limited by the spatial separation of the two main diffracted orders, which, because of the focusing of the incident light beam, is reached for a frequency separation δf of 3.5 MHz. Experiments have then been drawn with δf up to 28 MHz, which corresponds to $\Delta\phi_i = 8\pi$.

The experimental results are reported in Fig. 8 for total acousto-optic efficiencies of 5%, 30%, and 70%. The threshold value $\Delta\phi_t$ of the inverse phase mismatch depends on the acousto-optic efficiency. Its locus (L) then separates the curves in two regions, the left corresponding to the limitations of the phase-grating dynamic range and the right to the acoustic nonlinearities ones. It is seen that for efficiency up to 70%, the maximal value for $\Delta\phi_t$ is 6π. A good fit with the theoretical predictions has been found.

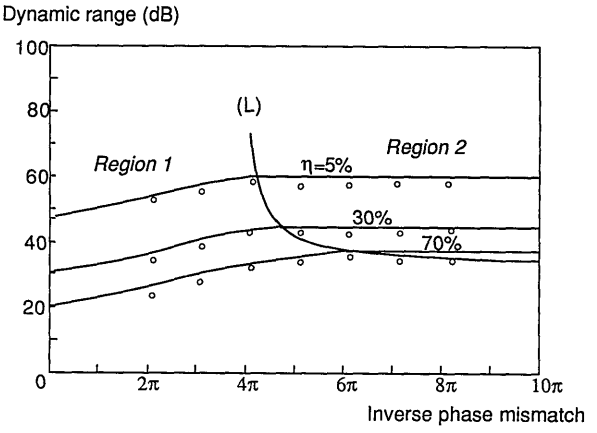

Fig. 8. Dynamic range versus inverse phase mismatch for different acousto-optic efficiencies. Region 1, phase-grating limitations; region 2, acoustic nonlinearities limitations; O, experimental data.

Conclusion

It has been shown that the phase-grating intermodulation products in multifrequency acousto-optic modulators can be significantly reduced with a proper anisotropic interaction configuration. Up to 16-dB enhancement of the dynamic range could be reached compared with the isotropic case. An original experimental protocol using heterodyne detection has been presented and is used to validate the theoretical predictions for a paratellurite multifrequency acousto-optic cell. Experimental results are in good agreement with theory.

Appendix A: Coupled-Wave Formalism for the Multifrequency Acousto-Optic Interaction

The classical coupled-wave equations[13] may be conveniently written, in the case of the bifrequency interaction described in this paper, as

$$\begin{aligned}
dg_0/dz &= -jc_1g_1 - jc_2g_2,\\
dg_1/dz &= -jc_1g_0 - jc_2g_{(1,2)}\exp(-j\Delta\phi_i z),\\
dg_2/dz &= -jc_2g_0 - jc_1g_{(2,1)}\exp(j\Delta\phi_i z),\\
dg_{(1,2)}/dz &= -jc_2g_1\exp(j\Delta\phi_i z)\\
&\quad - jc_1g_{(1,2,1)}\exp(j\Delta\phi_i z),\\
dg_{(2,1)}/dz &= -jc_1g_2\exp(-j\Delta\phi_i z)\\
&\quad - jc_2g_{(2,1,2)}\exp(-j\Delta\phi_i z),\\
dg_{(1,2,1)}/dz &= -jc_1g_{(1,2)}\exp(-j\Delta\phi_i z),\\
dg_{(2,1,2)}/dz &= -jc_2g_{(2,1)}\exp(j\Delta\phi_i z),
\end{aligned}$$

where the g terms refer to the complex amplitude of the electric displacement vector $\mathbf{D}$ related to the considered electromagnetic order. The incides 0, 1, 2, (1, 2), (2, 1), (1, 2, 1), and (2, 1, 2) have the same meaning as described in Fig. 4. The variable z is the reduced coordinate $z = x/w$ so that $0 < z < 1$ in the interaction region. The term $c_i (i = 1$ or 2) is related to the acoustical power P_i of the considered acoustic

carrier by

$$c_i = \frac{\pi}{2}\left(\frac{P_i}{P_0}\right)^{1/2},$$

where P_0 is the required power for 100% efficiency (single-tone Bragg regime) and is given by

$$P_0 = \frac{\lambda^2}{2M_2}\frac{H}{W},$$

H being the transducer height (the dimension normal to W).

References

1. D. L. Hecht, "Multifrequency acoustooptic diffraction," IEEE Trans. Sonics Ultrason. **SU-24,** 7–18 (1977).
2. G. Elston, "Intermodulation products in acoustooptic signal processing systems," in *Proceedings of the IEEE Ultrasonics Symposium,* B. R. McAvoy, ed. (Institute of Electrical and Electronics Engineers, New York, 1985), pp. 391–397.
3. I. C. Chang, "Multifrequency acoustooptic diffraction in wideband Bragg cells," in *Proceedings of the IEEE Ultrasonics Symposium,* B. R. McAvoy, (Institute of Electrical and Electronics Engineers, New York, 1983), pp. 445–449.
4. D. L. Hecht, G. Petrie, and S. Wofford, "Multifrequency acoustooptic diffraction in optically birefringent media," in *Proceedings of the IEEE Ultrasonics Symposium,* B. R. McAvoy, ed. (Institute of Electrical and Electronics Engineers, New York, 1979), pp. 46–50.
5. D. L. Hecht, T. Mannigel, J. Rieden, and M. Silver, "Wideband recording using acoustooptics," in *Proceedings of the IEEE Ultrasonics Symposium,* B. R. McAvoy, ed. (Institute of Electrical and Electronics Engineers, New York, 1973), pp. 112–116.
6. M. G. Moharam and L. Young, "Criterion for Bragg and Raman–Nath diffraction regimes," Appl. Opt. **17,** 1757–1759 (1978).
7. M. G. Gazalet, G. Waxin, J. M. Rouvaen, R. Torguet, and E. Bridoux, "Independent acoustooptic modulation of the two wavelengths of a bichromatic light beam," Appl. Opt. **23,** 674–681 (1984).
8. V. V. Lemanov and K. Yushin, "Nonlinear effects in the propagation of elastic waves in piezoelectric crystals," Sov. Phys. Solid State **15,** 2140–2141 (1974).
9. Y. Ohmachi, N. Uchida, and N. Nuzeki, "Acoustic wave propagation in TeO_2 single crystal," J. Acoust. Soc. Am. **51,** 164–167 (1972).
10. I. C. Chang, "Acoustooptic devices and applications," IEEE Trans. Sonics Ultrason. **SU-23,** 2–21 (1976).
11. T. Yano, M. Kawabuchi, A. Fukumoto, and A. Watanabe, "TeO_2 anisotropic Bragg light deflector without midband degeneracy," Appl. Phys. Lett. **26,** 689–691 (1975).
12. M. G. Gazalet, S. Carlier, J. P. Picault, G. Waxin, and C. Bruneel, "Multifrequency paratellurite acoustooptic modulators," Appl. Opt. **24,** 4435–4438 (1985).
13. J. M. Rouvaen, M. Ghazaleh, E. Bridoux, and R. Torguet, "On a general treatment of acousto-optic interactions in linear anisotropic crystals," J. Appl. Phys. **50,** 5472–5477 (1979).